Supplement of Biogeosciences, 13, 3319–3329, 2016
http://www.biogeosciences.net/13/3319/2016/
doi:10.5194/bg-13-3319-2016-supplement

Biogeosciences Open Access EGU

Supplement of

Temperature-mediated changes in microbial carbon use efficiency and ^{13}C discrimination

Christoph A. Lehmeier et al.

Correspondence to: Sharon A. Billings (sharon.billings@ku.edu)

Supplementary Material

Exploring the principle of chemical and isotopic equilibrium in an open flow-through system at steady-state

The basic idea of our approach is that the rate of CO_2 addition to the reactor headspace (Fig. 1) and the $\delta^{13}C$ of this CO_2 represent the respiration rate of the microbial population and the $\delta^{13}C$ of respired CO_2 at steady-state, respectively (Fig. 2). Steady-state here means that a bacterial population of constant size or density is growing at a constant rate, determined by the dilution rate of the reactor. The population then has a constant respiration rate, which is determined, in principle, by the specific environmental conditions at which the continuous flow reactor is operated.

The principle underlying this approach is based on established isotope theory, described in detail by Craig & Gordon (1965) and Fry (2006), and we are able to illustrate the validity of this principle with our experimental setup.

We had two gas cylinders, for which we directly measured concentration and $\delta^{13}C$ of the CO_2 with the $^{13}CO_2/^{12}CO_2$ analyzer via the flow path depicted in Supplementary Fig. 1. These measurements yielded that gas 1 had a CO_2 concentration of 302 ppm and a $\delta^{13}C$ of -13.2 ‰ and gas 2 had a CO_2 concentration of 1015 ppm and a $\delta^{13}C$ of -48.9 ‰.

We then installed the chemostat reactor into this flow path (Supplementary Fig. 2), in exactly the same way as in the experiments described in the main manuscript, just without the reservoir tank (compare with Fig. 1). We filled the reactor with approximately 1 liter of the same autoclaved

nutrient medium that we used in our experiments. The medium had a pH of 6.5, a temperature of 22.1 °C and was not inoculated with microorganisms.

We first expelled inorganic C from the reactor medium, which will have been prevalent mainly in the form of H_2CO_3 (aq) and HCO_3^- (Stumm and Morgan, 1981), by bubbling CO_2-free air through the medium for about 6 hours (Supplementary Fig. 3). As the CO_2 concentration in the reactor headspace approached zero ppm, its apparent $\delta^{13}C$ became more and more negative (Supplementary Fig. 3).

We then switched from CO_2-free air to gas 1, and let gas 1 bubble through the reactor medium for about 12 hours. Both concentration and $\delta^{13}C$ in the reactor headspace changed rapidly after the switch and gradually approached 302 ppm and -13.2 ‰, the same as determined for gas 1 by direct measurements (Supplementary Fig. 3; and see above).

The gradual increase in headspace CO_2 after switching from CO_2-free air to gas 1 reflects the build-up of H_2CO_3 (aq) and HCO_3^- pools in the nutrient medium which are strong sinks for CO_2. However, when they reached their final sizes (dictated by temperature and pH of the nutrient medium), they had no further net sink capacity as evidenced by the invariant headspace CO_2 concentration identical to that of the gas 1 bottle measured directly (Supplementary Figs. 1, 3). Thus, the system was in chemical equilibrium, which means that the H_2CO_3 (aq) and HCO_3^- pool sizes did not change anymore. The re-establishment of a constant $\delta^{13}C$ of reactor headspace CO_2 at the same value as obtained by direct measurement of the gas bottle proved that the system had also reached isotopic equilibrium, meaning that the $\delta^{13}C$ of the export flux (measured reactor headspace CO_2) was identical with the $\delta^{13}C$ of the import flux CO_2 (from the gas bottle; Supplementary Figs. 2, 3).

We then switched the gas supply from gas 1 to gas 2. Again, both concentration and $\delta^{13}C$ changed rapidly after the switch and gradually approached the values of the CO_2 measured directly, i.e. 1015 ppm and a $\delta^{13}C$ of -48.9 ‰ (Supplementary Fig. 3).

We then decreased the reactor temperature from 22.1 °C to 11.4 °C, a temperature range similar to that used in the experiments of the main manuscript. Both sizes and fractionation factors of the carbonate pool system must have reacted (Vogel et al., 1970; Mook et al., 1974; Stumm and Morgan, 1981; Szaran, 1997), and due to the slow and gradual change in reactor temperature, this translated into slow adjustments in reactor headspace CO_2 concentration and $\delta^{13}C$ (Supplementary Fig. 3). However, twelve hours after initiation of the temperature change, the chemical and isotopic equilibria were re-established.

We then injected 2.5 mL of acetic acid ($C_2H_4O_2$) into the nutrient medium which caused a change in pH from 6.5 to 3.45. Both concentration and $\delta^{13}C$ of reactor headspace CO_2 responded rapidly, as both sizes and fractionation factors of the carbonate pool system will have adjusted to the new pH. However, both concentration and $\delta^{13}C$ of reactor headspace CO_2 again returned to the values of the gas bottle within a few hours, again proving that a new steady-state of chemical and isotopic equilibrium was established.

At these three steady-states when bubbling gas 2, there will have been more or less pronounced differences in the sizes and the isotopic signatures of the inorganic C pools, caused by temperature and pH effects (Vogel et al., 1970; Mook et al., 1974; Stumm and Morgan, 1981; Szaran, 1997), but this did not change the fact that in this open flow-through system, concentration and $\delta^{13}C$ of the import fluxes was the same as that of the export fluxes at steady-state.

In the chemostat experiments described in the main manuscript, we used this principle. Essentially, the only difference was that the source of CO_2 entering the reactor was not a gas bottle, but respiratory activity of a microbial population.

In our chemostat runs ranging from 13 °C to 26.5 °C, there will have been some differences in size and isotopic composition of the inorganic C pools, but they were irrelevant for the principle that what is going into the reactor is what is going out of the reactor, both in terms of respiration rate, as well as of $\delta^{13}C$ of respired CO_2.

Supplementary Figure 1: Flow-path to measure gas from a cylinder with a $^{13}CO_2/^{12}CO_2$ analyzer. See explanations in Supplementary Material and compare with Fig. 1 in the main manuscript.

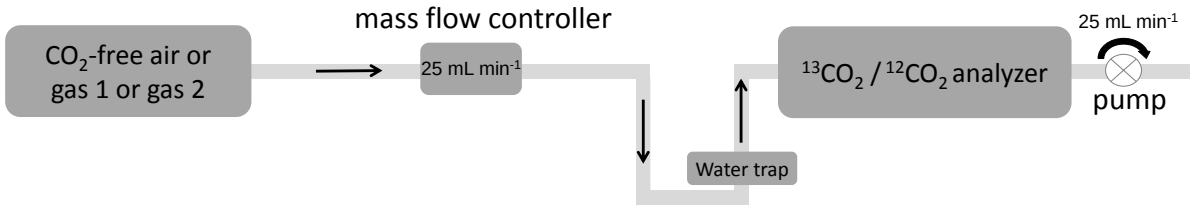

Supplementary Figure 2: Flow-path to measure cylinder gas bubbling through a sterile nutrient medium with a $^{13}CO_2/^{12}CO_2$ analyzer. See explanations in the Supplementary Material and compare with Fig. 1 in the main manuscript.

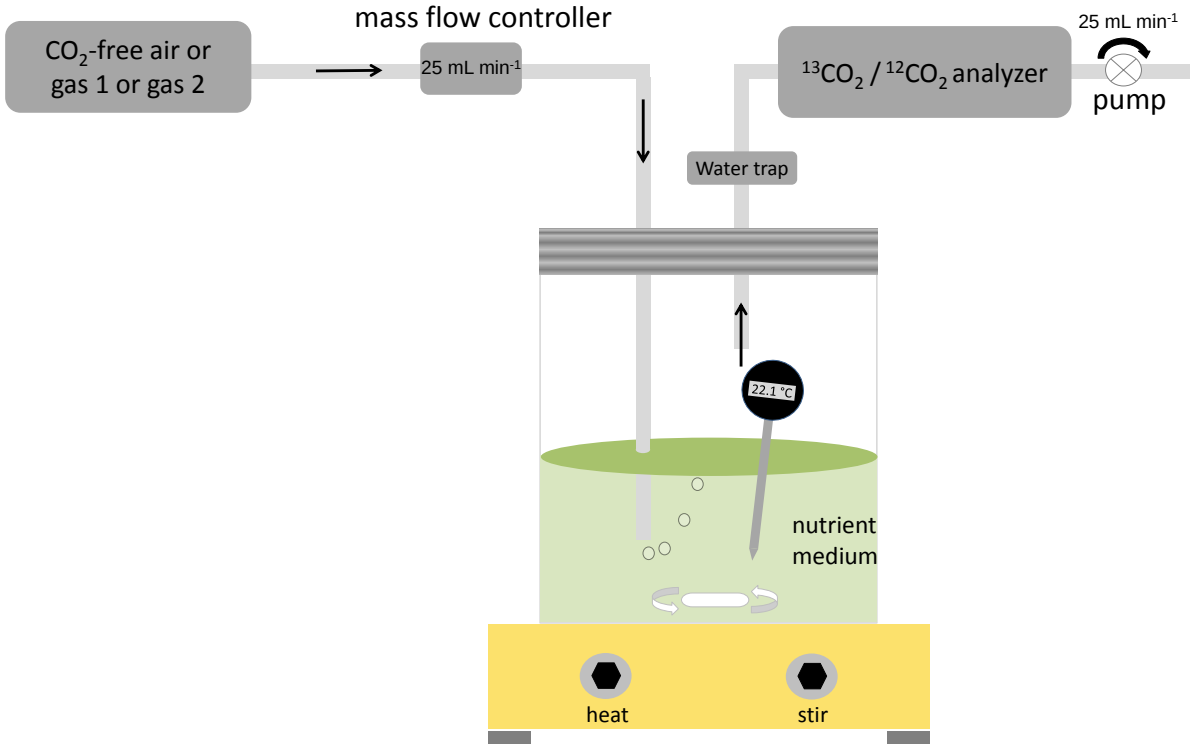

Supplementary Figure 3: Time course of CO_2 concentration and $\delta^{13}C$ measurements using the experimental system depicted in Supplementary Fig. 2. See Supplementary Material for a detailed description.

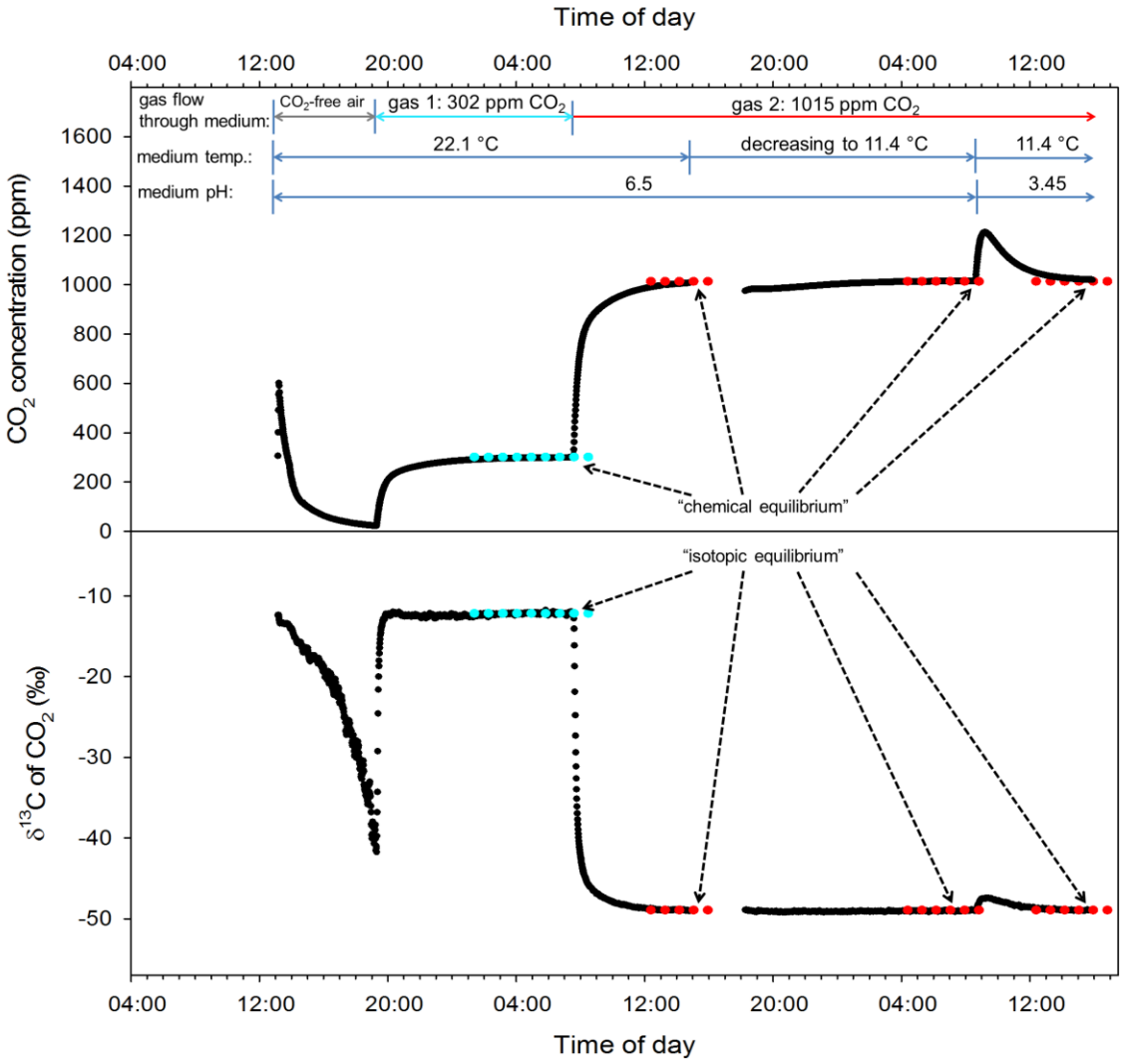

Supplementary Table 1. Process and growth parameters of independent continuous-culture chemostat runs with *P. fluorescens* at steady-state, performed at seven different temperatures of the reactor medium. Reactor biomass, %C and %N in biomass and biomass C:N were obtained by elemental analysis of microbial dry matter, filtered from reactor medium with 0.2 µm filters (n=4, but n=2 for 26.5 °C). Errors given are 1 SD.

reactor temperature (°C)	reactor volume (mL)	medium flow rate (mL h^{-1})	reactor half-life (h)	%C in biomass	%N in biomass	C:N ratio in biomass (w:w)
13	785	115.5	4.7	28.0 ± 1.1	7.9 ± 0.4	3.5
14.5	950	120	5.5	28.6 ± 0.3	7.6 ± 0.3	3.7
16	820	120	4.7	29.0 ± 0.6	8.4 ± 0.3	3.4
18	910	121	5.2	27.8 ± 0.9	7.7 ± 0.1	3.6
21	920	118	5.4	27.1 ± 0.5	7.9 ± 0.1	3.4
23.5	835	112	5.2	27.3 ± 0.2	6.9 ± 0.2	4.0
26.5	865	122	4.9	27.7 ± 0.1	7.8 ± 0.1	3.5

99